Supplementary Information (SI) for Journal of Materials Chemistry A.

Supporting Information for:

Construction of waffle-like NS-ZIF@V_2CT_x heterostructures for high-performance potassium ion batteries

Yue Qin [a], Weifang Zhao [b*], Ting Wang [a], Wenlong Liu [a], Tengfei Zhou [c], Xiaole Han [a], Yi Liu [a], Juncheng Hu [a], Qingqing Jiang [a*]

[a] Key Laboratory of Catalysis and Energy Materials Chemistry of Ministry of Education, School of Chemistry and Materials Science, South-Central Minzu University, Wuhan 430074, China

[b] Ganfeng Li Energy Technology Co., Ltd., Xinyu 338000, Jiangxi, China

[c] Institutes of Physical Science and Information Technology, Anhui University, Hefei 230601, China

1. Experimental Method

1.1 Materials

The materials used here include:V_2AlC (98 wt%, 400 mesh, Ichiyi Technology Co. Ltd.), TMAOH (tetramethylammonium hydroxide, 25 wt%, Macklin Co. Ltd.), methanol (99.5%), polyvinylpyrrolidone (PVP, GR), and ascorbic acid were purchased from Sinopharm Chemical Reagent Co. HCl (36-38 wt%), $Zn(NO_3)_2$-$6H_2O$ (99.99%), $Co(NO_3)_2$-$6H_2O$ (99.99%), dimethylimidazole (98%), potassium metal from potassium ion batteries (K,99.9%),1,2-dimethoxyethane (DME, AR, 99.5%) and potassium bis(fluorosulfonyl)imide (KFSI, AR, > 95%) were purchased from Aladdin Industries.

1.2 Materials characterization

The morphology of the resulting products was observed and photographed using a scanning electron microscope (SEM) (Hitachi SU-8010, Japan) at a deceleration voltage of 1.5 kV. Transmission electron microscopy images were taken using a JEOL JEM-2010 LaB_6 high-resolution transmission electron microscope (200 kV). High resolution transmission electron microscopy (HRTEM) images were taken using a JEOL JEM-2100F field emission high resolution transmission electron microscope at 200 kV. X-ray diffraction (XRD) patterns were recorded using a Bruker AXS D8 Advance X-ray diffractometer with a cu-k-α radiation source (λ = 1.5406 Å). Raman spectra were collected using a DXR Raman confocal microscope (Thermo Fisher Scientific, USA), 532 nm @10 mW laser. X-ray photoelectron spectroscopy (XPS) measurements were performed using Al Kα radiation as the excitation source (VG Multilab 2000 Photoelectron Spectrometer, 2 × 10-6 Pa vacuum).

1.3 Electrochemical characterization

A CR2032 button cell was selected to test various electrochemical properties. The mixtures consisted of prepared material (70 wt%), polyvinylidene fluoride (PVDF, 10 wt%) and cochineal black (20 wt%). The mixtures were then applied to a copper foil (collector) to prepare V_2CT_x, ZIF@V_2CT_x and NS-ZIF@V_2CT_x electrodes (mass loadings of 0.2 mg cm^{-2} and diameters of 8 mm). Potassium metal foil was used as the reference electrode for the assembly of the semi-PIBs, and polypropylene membranes (Celgard 2400) were used for the separator. The electrolyte was selected as 3 M KFSI (DME) and 200 μL of each CR2032 button cell was used.Charge-discharge tests and GITT tests were performed using a NEWARE battery tester (0.01-3 V, room temperature). CV (0.01 - 3 V, room temperature, 0.1 mV s^{-1} ~ 1.0 mV s^{-1}) and EIS spectra (5 mV, 0.01 Hz ~ 100 kHz) tests were performed on the IviumStathtype electrochemical workstation.

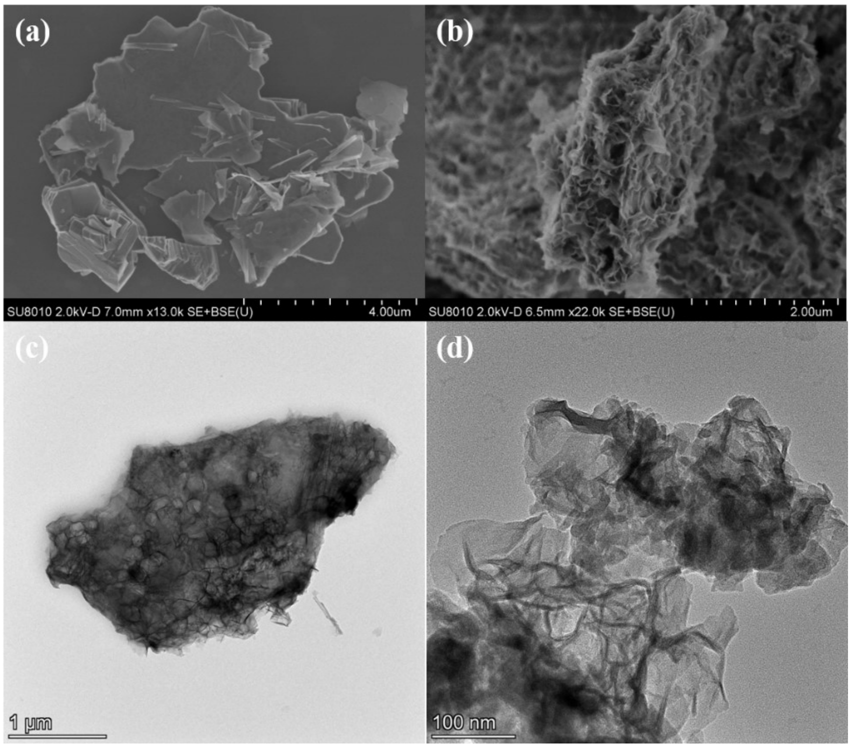

Figure S1. SEM images of (a) V_2CT_x, (b) NS-ZIF@V_2CT_x, TEM images of (c) NS-ZIF@V_2CT_x, and (d) NS-ZIF

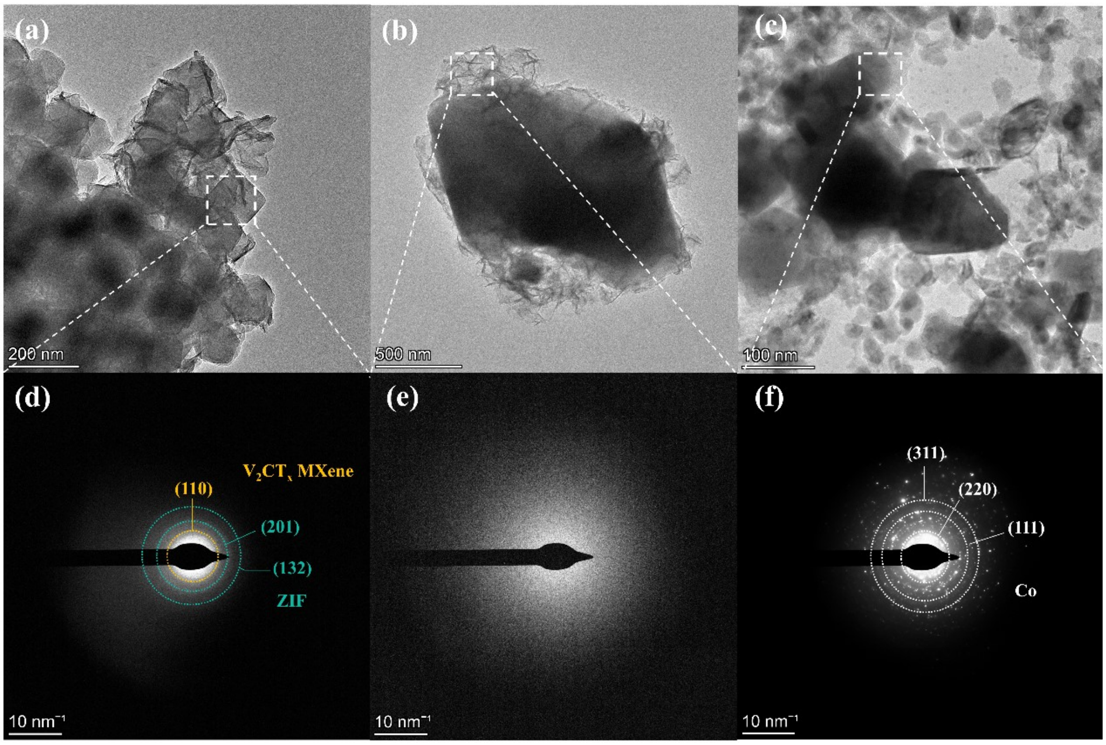

Figure S2. TEM images (a) ZIF@V_2CT_x, (b) NS-ZIF@V_2CT_x , (c) ANS-ZIF@V_2CT_x, SAED diffraction pattern of (d) ZIF@V_2CT_x, (e) NS-ZIF@V_2CT_x, (f) ANS-ZIF@V_2CT_x.

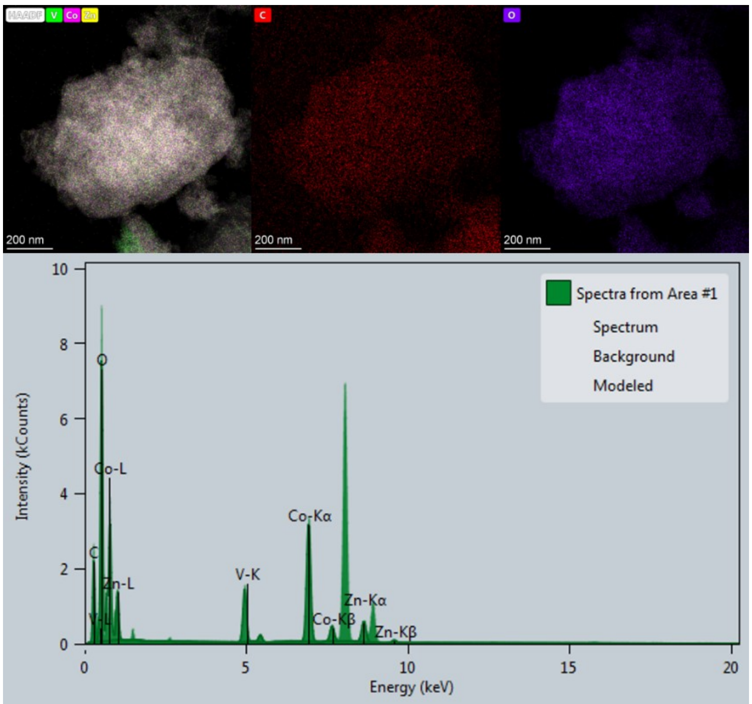

Figure S3. EDS elemental analysis map of NS-ZIF@V_2CT_x.

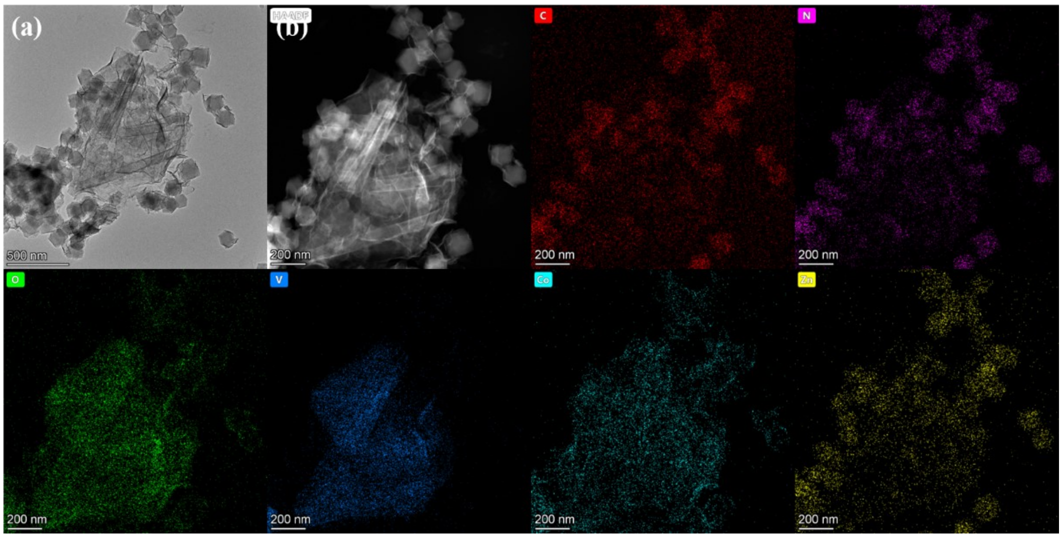

Figure S4. (a) TEM image, (b) EDS image of ZIF@V_2CT_x.

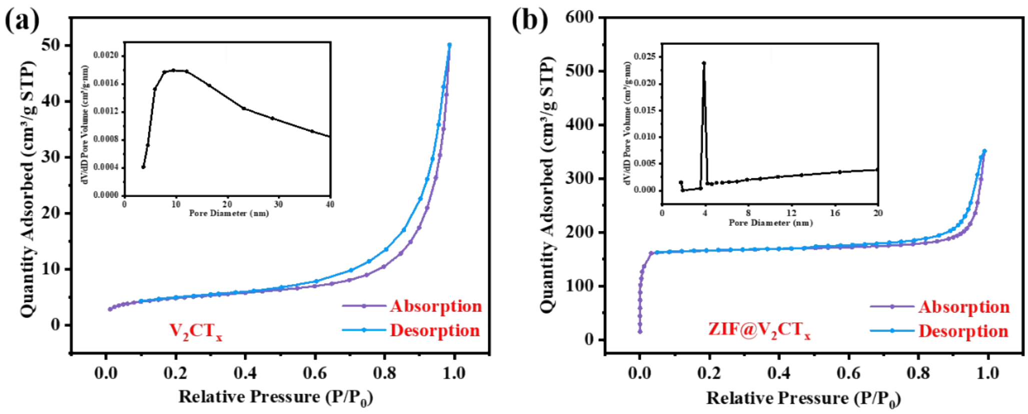

Figure S5. N_2 adsorption-desorption isotherms and pore size distribution of (a) V_2CT_x, and (b) ZIF@V_2CT_x.

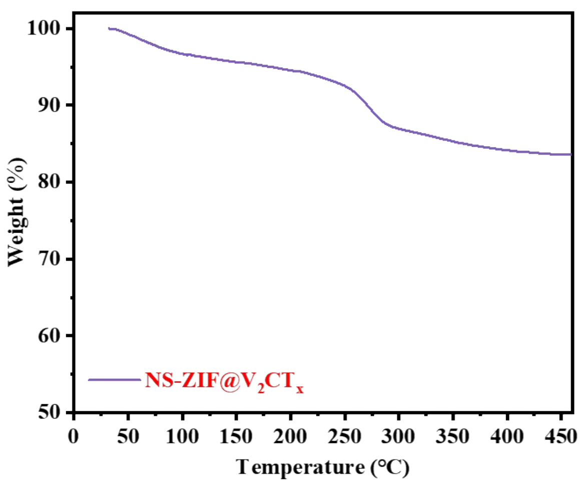

Figure S6. Thermogravimetric curve of NS-ZIF@V_2CT_x.

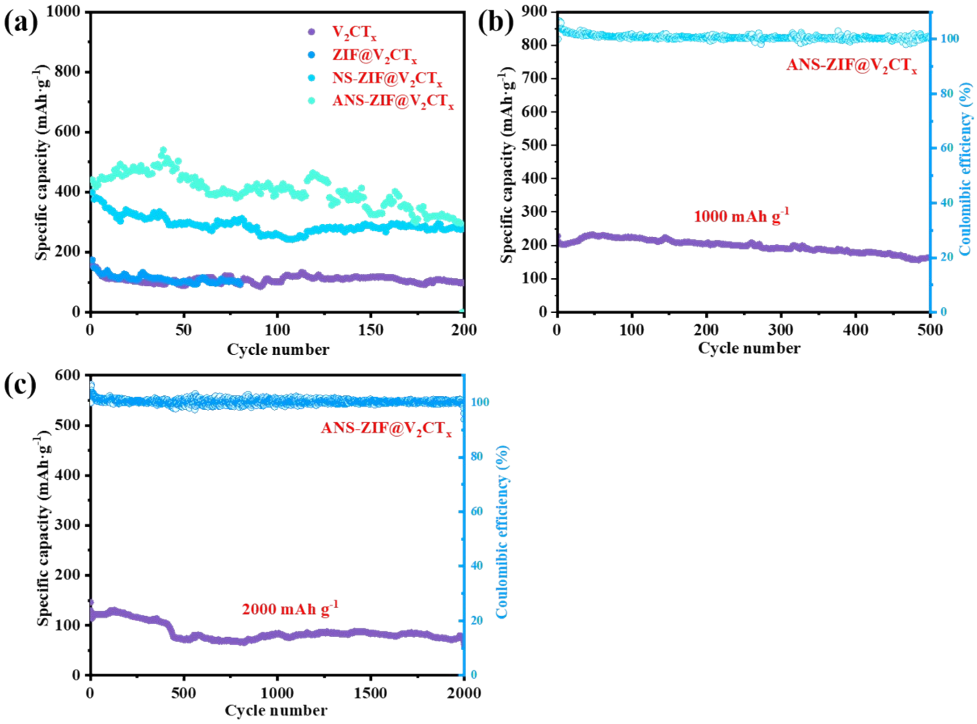

Figure S7. (a) Cycling performance of V_2CT_x, $ZIF@V_2CT_x$, $NS-ZIF@V_2CT_x$, and NS-ZIF@ V_2CT_x electrodes at current density of 100 mA g^{-1}, Cycling performance of ANS-ZIF@V$_2$CTx electrode at (b) 1000 mA g^{-1} and (c) 2000 mA g^{-1}.

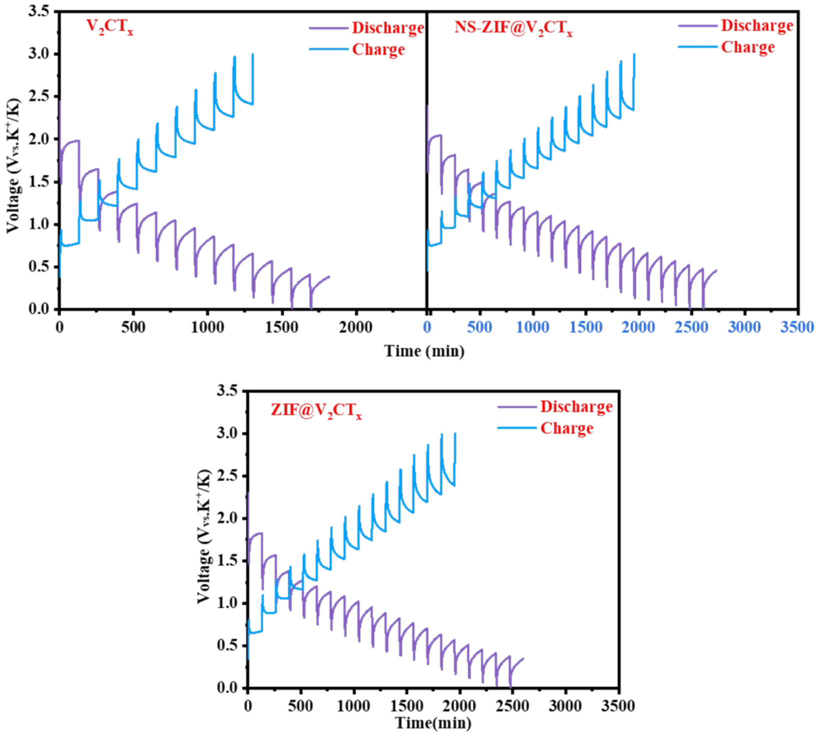

Figure S8. GITT plots of V_2CT_x, $NS-ZIF@V_2CT_x$ and $ZIF@V_2CT_x$.

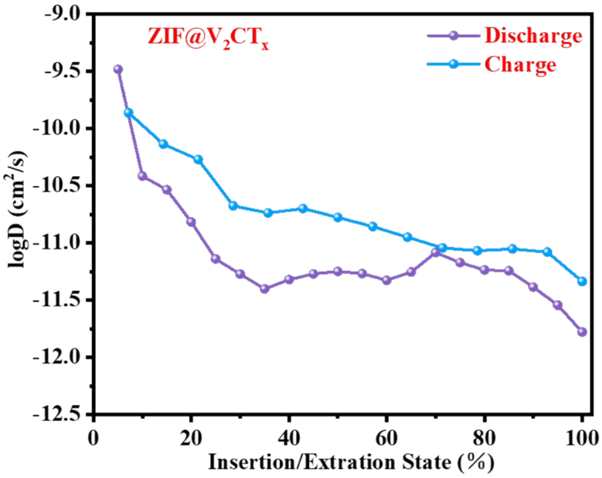

Figure S9. The calculated diffusion coefficient (D_{K^+}) of ZIF@V_2CT_x electrode.

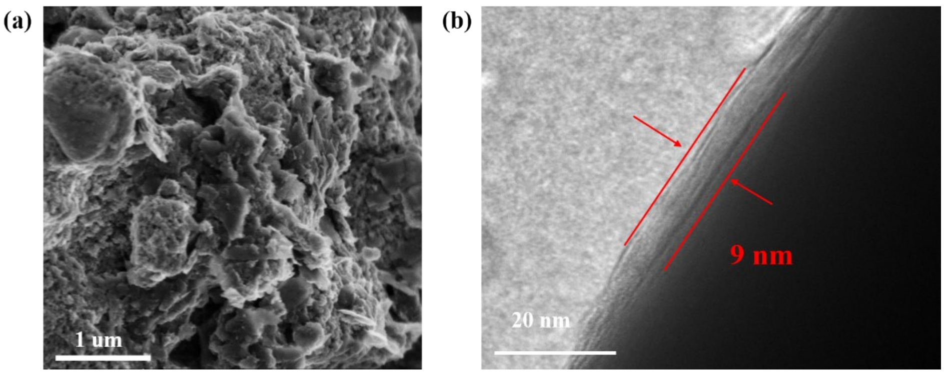

Figure S10. (a) SEM image of NS-ZIF@V_2CT_x electrode and (b) TEM image of SEI layer after 200th charge/discharge cycles.

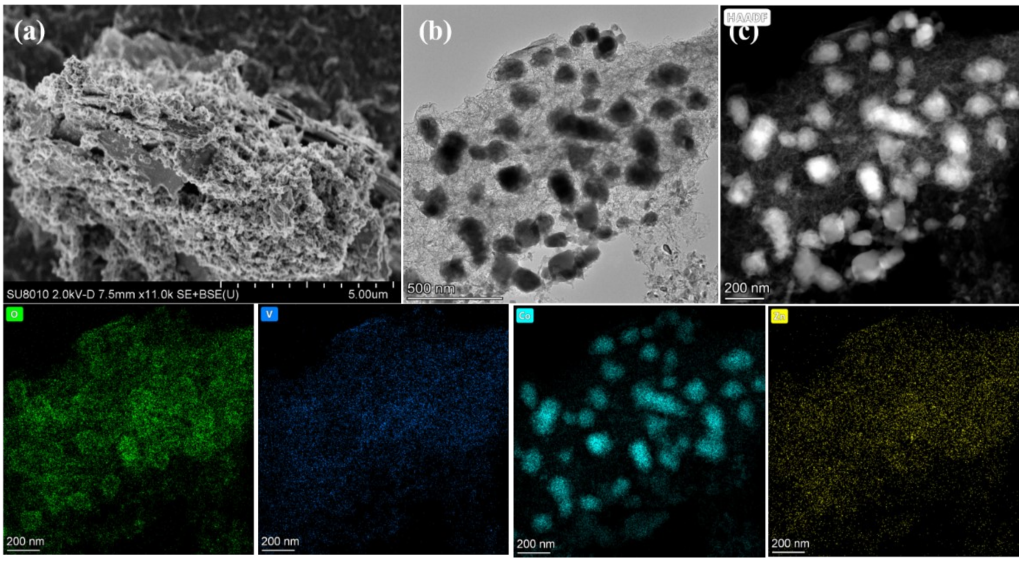

Figure S11. (a) SEM, (b) TEM, (c) EDS of ANS-ZIF@V_2CT_x samples.

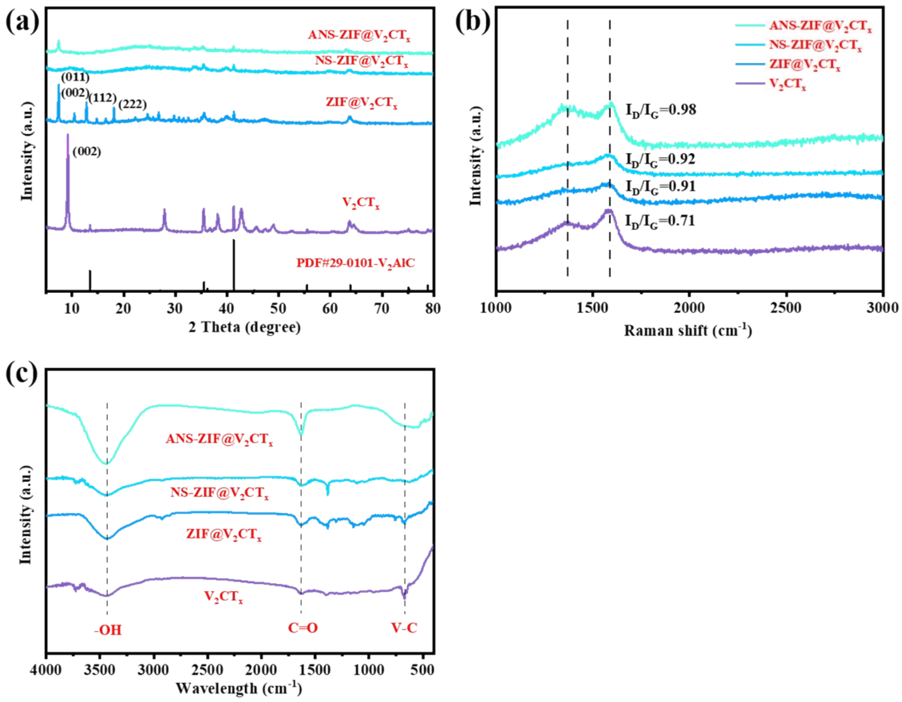

Figure S12. (a) XRD patterns, (b) Raman spectra, (c) FT-IR spectra of V_2CT_x, ZIF@V_2CT_x, NS-ZIF@V_2CT_x, and NS-ZIF@ V_2CT_x.

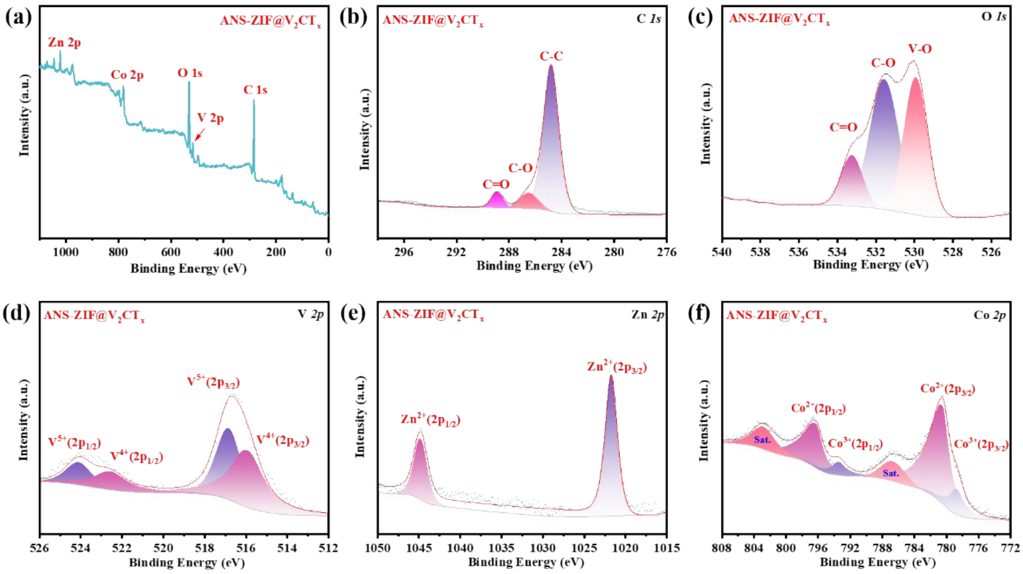

Figure S13. XPS data for ANS-ZIF@V_2CT_x sample of (a) XPS survey, (b) C 1s, (c) O1s, (d) V 2p, (e) Zn 2p, and (f) Co 2p spectrum.

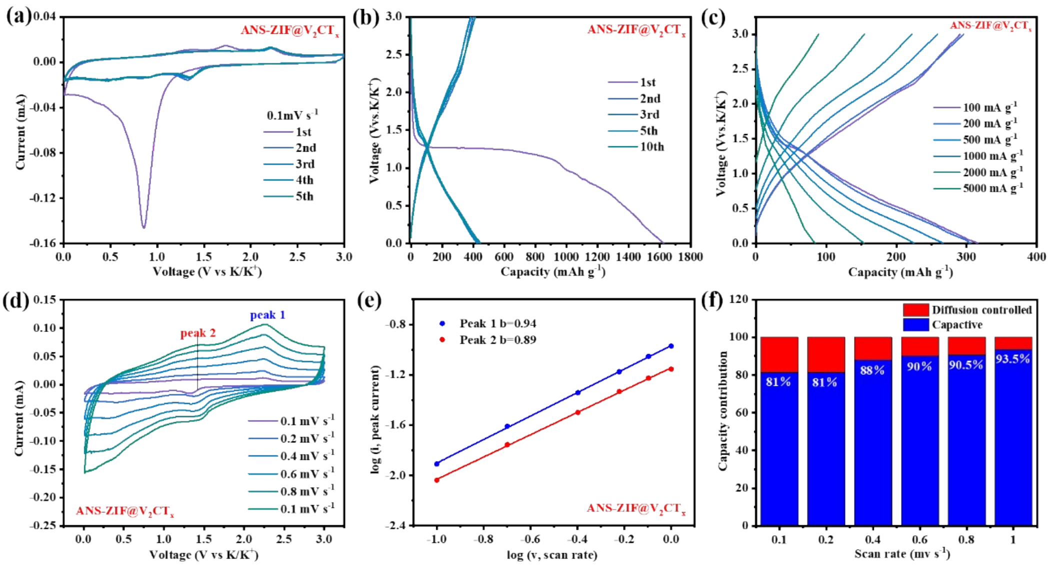

Figure S14. (a) CV curves, (b) GCD profiles, (c) GDV profiles, (d) CV curves at different sweep speeds, (e) anode peaks corresponding to the b-value, and (f) capacitive contributions of ANS-ZIF@V_2CT_x electrode.

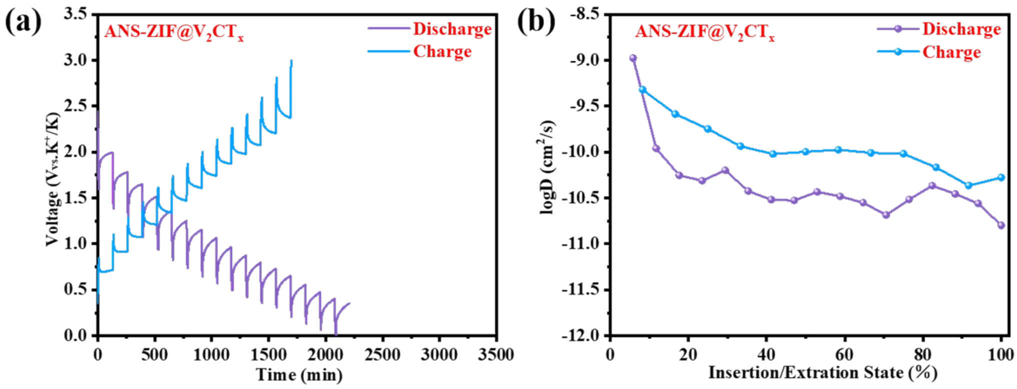

Figure S15. (a) GITT test, (b) the calculated diffusion coefficient (D_{K^+}) of ZIF@V_2CT_x electrode.

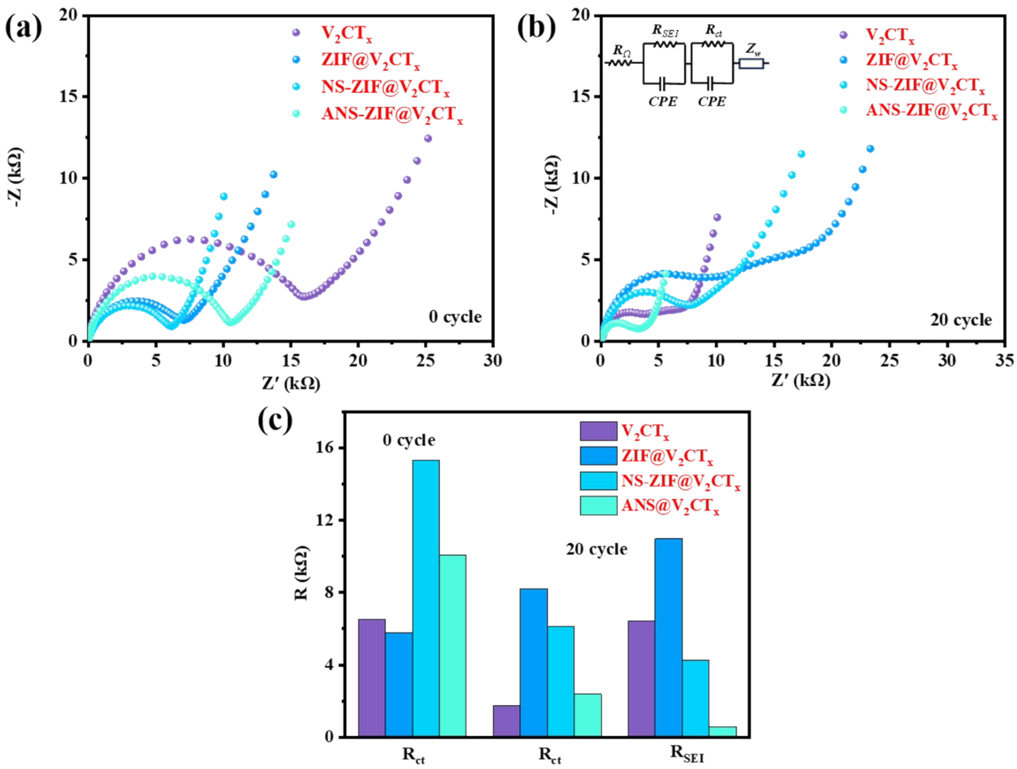

Figure S16. Plots of EIS data for (a) 0 cycles of EIS, (b) after 20 cycles of, and (c) the simulated R_{ct}, and R_{SEI} values.